2014 IEEE International Conference on Robotics & Automation (ICRA)
Hong Kong Convention and Exhibition Center
May 31 - June 7, 2014. Hong Kong, China

Characteristics Analysis and Mechanical Implementation of Human Finger Movements

Wenrui Chen, Caihua Xiong, Mingjin Liu, and Liu Mao

***Abstract*—How to design a robotic hand reflecting human hand motion information as much as possible is a constantly exploring problem. In this paper, we propose an approach to mechanical design of compliant underactuated finger for prosthetic hand based on the decomposition of human hand movements. Hand movements are decomposed into primary and secondary motion in PCA coordinate system. The primary motion is achieved in free motion via actuators, and the secondary motion is implemented with mechanical compliance matching statistics characteristic of human motion data. Although analysis and design of single finger is always throughout this paper, the same method can be generalized to the whole hand design and the parameters design of other mechanical configuration.**

I. Introduction

One of the challenging problems in robotics is implementtation of human-like movements in unstructured human environment. It is difficult to replicate the function of human hand, because of the complicated anatomical structure and mysterious neuromuscular control system. One approach to reduce this complexity is through *synergy*, which is from neuroscience and shows that a continuous subspace of configuration space can be used to approximate everyday human hand tasks.

Santello et al. [1] investigated grasping poses from mime grasps for a large set of familiar objects via principal components analysis (PCA) and revealed that more than 80% of hand posture information is contained in the first two principal components, which shows that the grasping posture can be expressed as a much lower-dimensional subspace of the hand joint space and reflects significant joint coupling and inter-finger coordination. A similar rule about hand motion during grasping was discovered in subsequent research [2].

Human hand synergy provides a natural modeling paradigm for robotics. Ciocarlie and Allen [3] used the idea to exploit the dimensionality reduction in problems of automated grasp synthesis, and has been applied effectively to derive pre-grasp shapes for a number of complex robotic hands. Brown and Asada [4] designed a mechanical hand in which more or less accurate actuators are connected to different groups of mechanically interconnected joints, with a priority inspired by resemblance to postural synergies observed in human hands.

Brown and Asada [4] designed the mechanical hand to replicate the lower-order synergies and ignore higher-order principal components. Introducing a model of compliance in rigid-body system to solve force indeterminacies, Bicchi et al. [5, 6] did not give the method to design parameters but showed quality of grasp is quite robust with respect to parameter values. The synergy approach to the mechanical design of anthropopathic hand can greatly reduce the number of actuators and simplify the control strategy, but it also brings new issues. The postural synergies, i.e. the first few principal components, account for vast majority of hand posture information. However, even though they are small, higher-order principal components do not represent random variability but instead provide additional information about the object [2]. How to design anthropopathic hands to retain high-order information while implementing the principal motion is a difficult problem.

In this paper, the approach to embed human hand movement information into robotic hand mechanism is studied. In contrast to the grasp measure of hand such as force distribution, force-closure [5] and robust [7], we are interested in the motion of robotic hand imitating human hand. In particular, we examine the motion characteristics of index finger and implement it in mechanic finger. In different grasp patterns (such as power, precision, lateral, etc.), there are significant independence between and among each finger, and the single finger is allowed visual representation and detailed analysis, which is difficult for the whole hand with more than twenty DOFs [8] [9].

In the work presented in this paper, we extract human finger movement characteristics with PCA and analyze the finger movement behavior in PCA coordinate system, which is emulated using tendon-pulley mechanism. Then, compliance substituted for higher-order principal motions, we propose a quantitative method of mechanical implementing anthropomorphic posture synergy and compliance, and accordingly present a novel anthropopathic fingers which can be embedded in prosthetic hands.

II. Human Finger Movements

We hope to provide methodological guidance for prosthetic hand design through analysis of human hand motion data. Therefore, the three-joints finger, easy to visualized analysis, will be analyzed as an example to elicit our design ideas.

A. Acquisition of human movement data

The human hand permits an infinite number of different trajectories to move the fingers from one location in space to

*Resrach supported by the National Basic Research Program of China (973 Program) (Grant No. 2011CB013301), the National Science Fund for Distinguished Young Scholars of China (Grant No. 51025518), and the State Key Program of National Natural Science of China (Grant No. 51335004).

Wenrui Chen, Caihua Xiong, Mingjin Liu, and Liu Mao are with School of Mechanical Science and Engineering, Huazhong University of Science and Technology, Wuhan, 432700, China (e-mail: {chenwenrui, chxiong, mjliu, maoliu}@hust.edu.cn).

another. It is this ability that makes the hand so valuable in many daily tasks, especially grasp and manipulation. Attempts to formalize human tendency to simplify the space of possible grasps can be traced back to Napier's pioneering grasp taxonomy [10], which would divide grasps into power and precision grasps. In studying the grasps required for manufacturing tasks, Cutkosky showed a grasp hierarchy which offers a classification scheme for typical human grasps [11]. In [12], Fiex reviewed a large field of work on grasp taxonomies and provided a much more comprehensive and detailed organization of human grasps. Grasp types divided elaborately more and more are not equally important, some grasp often used in our daily life, and some not so. An investigation of the frequency of use of various grasp types in daily activities is presented in [13]. The average durations and frequencies for the top 10 grasps, which account for approximately 80% percent of the total grasp duration [14]. An optimal grasp set which can effectively handle as many different objects as possible was picked with the grasp span metric [15].

Synthesize the frequencies [14] and the grasp span metric [15], we choice 8 grasp types in Fiex grasp taxonomy involving the three main clusters, i.e. power, intermediate and precision grasps, as Fig. 1.

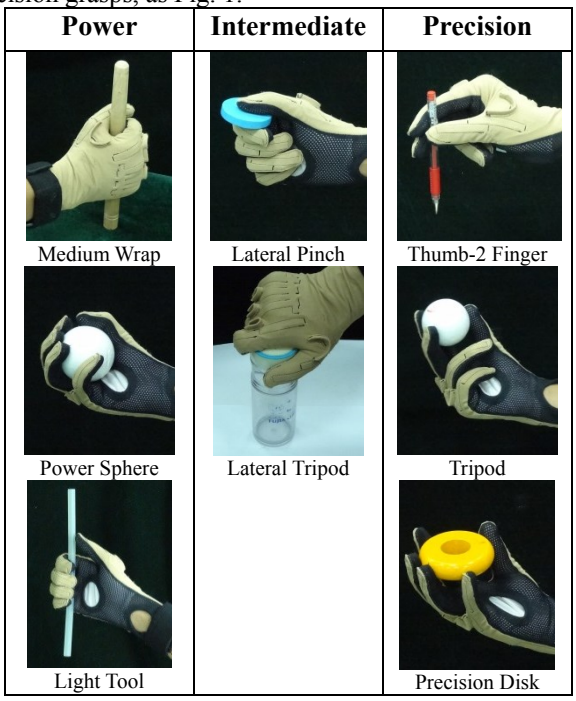

Fig. 1. The most ordinary using eight grasp types, which are used for data acquisition.

We measured the angles at the metacarpalphalangeal (MCP), proximal interphalangeal (PIP) and distal interphalangeal (DIP) joints of the four fingers. Flexion was defined as positive; the joint angles were defined as 0° when the finger was straight and in the plane of the palm. Using a Cyberglove, we collected joint angle reach-to-grasp data on 8 different grasps. After normalizing the duration of each movement, we analyzed the hand postures during this interval using PCA.

B. Characteristics analysis of index finger

Experimental data $\mathbf{X} \in \mathbf{R}^{n\times 3}$, blue point cloud in Fig. 2, is three-joints reach-to-grasp movements data of the single finger data on 8 different grasps, where n is the number of samples, and three joint angle, $\mathbf{q} = \begin{bmatrix} q_1 & q_2 & q_3 \end{bmatrix}^T$, is obtained in each sample.

Once the vector $\bar{\mathbf{q}}$ representing the mean hand position in the grasp configurations space has been computed, the PCA has been performed on the covariance matrix

$$\mathbf{S} = \frac{1}{n-1} \tilde{\mathbf{X}}^T \tilde{\mathbf{X}}, \tag{1}$$

where the centered data are $\tilde{\mathbf{X}} = \left\{ x_{ij} - \bar{q}_j \,|\, i = 1,...,n, j = 1,2,3 \right\}$. The characteristics of data distribution can be represented via constant density ellipsoid described in equation as

$$\left(\mathbf{q} - \bar{\mathbf{q}}\right)^T \mathbf{S}^{-1} \left(\mathbf{q} - \bar{\mathbf{q}}\right) = c^2, \tag{2}$$

where c is constant. The symmetric matrix S is diagonalized by an orthogonal matrix of its eigenvectors, $\mathbf{S} = \mathbf{PDP}^T$, where D is a diagonal matrix and P is a matrix of eigenvectors of S arranged as columns. The eigenvectors $\mathbf{p}_i$ is the direction of constant density ellipsoid spindle, and the eigenvalues d_{ii} is squared length of corresponding spindle. The data distribution characteristics of index finger joints can be expressed as Fig 2, where the blue point cloud is the joint angle sampling data.

The second and third principal components (PCs) are far less than the first PC, PC1> 85%. Three principal components in the movement direction are projected in Cartesian space as shown in Fig 3. Whether in joint space or in Cartesian space, it is obvious that the direction of the first PC is the main direction of movement, reflecting the general trend of finger movement, and the second and third PCs reflect the deviation degree from the main direction of movement in different directions.

To provide a vivid performance for the linear motion feature of the three PCs, a finger is designed with tendon-pulley transmission mechanism shown in Fig. 4. Three groups of pulleys are independently driven by three motors, and the radius ratio of each set pulleys equal to the proportions among corresponding elements of eigenvector. Then the three PCs of finger movement can be achieved separately by the three motors. Motor 1 synchronous bend three joints proportionally to achieve the first PC movement; motor 2 led q_1 and q_2 reverse movement and q_2 and q_3 conjugate movement, to achieve the second PC movement; motor 3 drive q_2 and q_3 reverse movement, but don't drive q_1, to achieve the third component.

In the data analysis, we found that the first element of PC3 is very close to zero. In other words, the plane spanned by PC1 and PC2, bearing 98% of the motion information, parallel to q_1 axis of the original coordinates. Therefore, with the two motor driving a finger, the coupling of q_2 and q_3 statistically meet the human hand law of motion. However, it is still too much for each finger flexion and extension movements of the practical robot hand by the two motors. Here we will introduce a mechanical implementation approach to achieve finger anthropomorphic movement with a single motor.

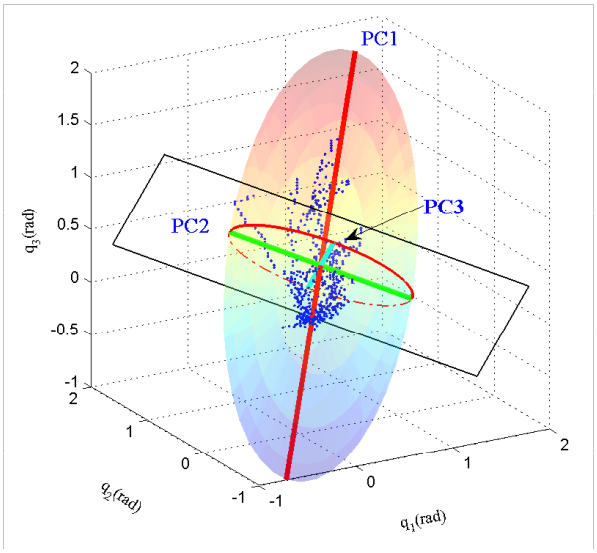

Fig. 2. Index finger movement data and its PCA characteristics

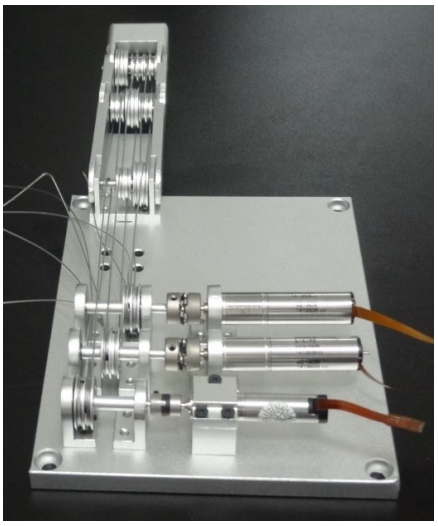

Fig. 4. PCA finger whose three PCs achieved separately by the three motors.

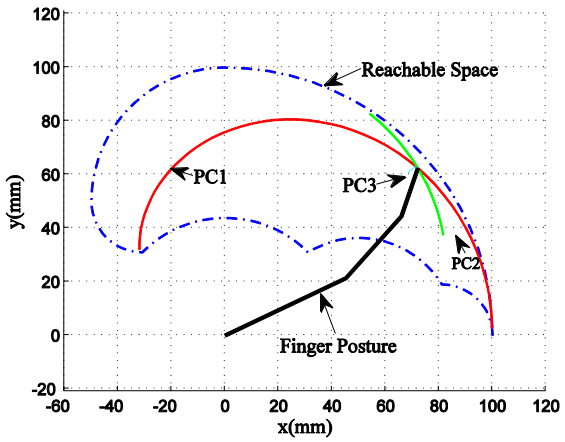

Fig. 3. Three principal components in Cartesian space projected from joint space.

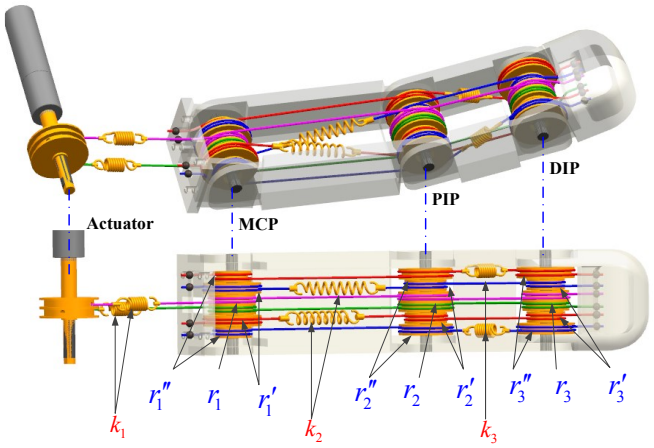

Fig. 5. Single-actuator PCA finger embedded mechanical compliance.

III. Mechanical Implementation

Previously, the characteristics of human finger movement data are extracted via PCA; and the finger mechanism is designed to achieve the PCs movement. We will reduce motors to one, while preserving more information in the finger mechanism.

A. Compliance embed

In three separate motors , motor 1 drives the first PC movement, is *primary motion* and will be reserved, while motors 2 and 3 drive movements in the plane spanned by PC2 and PC3 regulating gestures to achieve the different objects crawl, is *secondary motion*. We use mechanical compliance instead of motors 2 and 3 to achieve secondary motion. The most direct approach is to replace the motor with elastic elements, and the elastic element parameters reflecting the distribution of motion data. The original intention is that the mechanical compliance, which reflects how easily to motion in response to the same applied force, corresponds to the discrete level of movement data.

The movement ability along direction of PC2 and PC3 is different, manifested statistically as different variance along different directions. In the finger embedding elastic element in Fig. 5, the movement ability along the direction of PC2 and PC3 is showed as compliance, i.e. reciprocal of the rigidity. Therefore, compliance of mechanism is proportional to the variance of the motion data along PC2 and PC3 direction to achieve the movement ability matching, expressed as

$$k_3 / k_2 = \sqrt{d_{22}} / \sqrt{d_{33}} \qquad (3)$$

The relative value of elastic elements is given in (3), while their absolute sizes are associated with the other indicators of the finger, such as the performance of drive and the grasping force etc, which are also very important issues but not emphasis of this study.

B. Mechanical compliance matching to PCA

The aforementioned design methodology can be summarized in two steps: first, the lower-order principal components movement information of human hand is achieved through actuators; second, the higher-order principal components movement is achieved through the method of

mechanical compliance. In the second step, this design thought is essentially matching compliant ellipsoid of robotic hand mechanism and constant density ellipsoid of human motion data in the subspace of secondary motion.

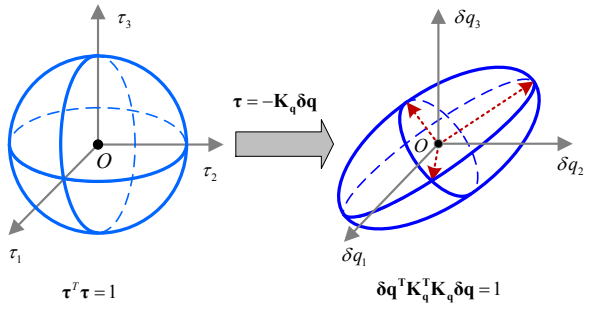

Fig. 6. Mapping the unit force sphere to compliance ellipsoid.

In the joint space, the set of unit force vector form the unit force sphere, denoted as

$$\boldsymbol{\tau}^T\boldsymbol{\tau} = 1. \tag{4}$$

The joint force $\boldsymbol{\tau}$ effects on joint and makes joint displacement $\delta\mathbf{q}$, whose relationship is expressed as

$$\boldsymbol{\tau} = -\mathbf{K}_q\delta\mathbf{q}, \tag{5}$$

where $\mathbf{K}_q$ is the stiffness matrix of joint space. $\mathbf{K}_q$ maps the unit force sphere to an ellipsoid of displacement, as illustrated in Fig. 6. Substituting (5) into (4), the mapped ellipsoid of displacement will be expressed as

$$\delta\mathbf{q}^T\mathbf{K}_q^T\mathbf{K}_q\delta\mathbf{q} = 1, \tag{6}$$

which is referred to as compliance ellipsoid. The compliance ellipsoid reflects the deformation of the joint space in different directions under the action of external force.

We decouple stiffness matrix in PCA coordinate system to achieve compliance ellipsoid and constant density ellipsoid matching.

According to the hand primary and secondary movement, joint space is broken into two subspaces and the base coordinates of PCA coordinate system is made up of two parts, $\mathbf{P} = [\mathbf{P}_p \quad \mathbf{P}_s]$, where $\mathbf{P}_p$ is the base of primary movement subspace and $\mathbf{P}_s$ is the base of secondary movement subspace.

In PCA coordinate system, the stiffness is expressed as

$$\mathbf{K}_{pca} = \mathbf{P}^T\mathbf{K}_q\mathbf{P}, \tag{7}$$

and the matrix of compliance ellipsoid can be expressed as

$$\mathbf{M}_{pca} = \mathbf{K}_{pca}^T\mathbf{K}_{pca} = \begin{bmatrix} \mathbf{M}_p & \mathbf{M}_{p.s}^T \\ \mathbf{M}_{p.s} & \mathbf{M}_s \end{bmatrix} \tag{8}$$

where

$$\mathbf{M}_p = \mathbf{P}_p^T\mathbf{K}_q^T\mathbf{K}_q\mathbf{P}_p$$
$$\mathbf{M}_s = \mathbf{P}_s^T\mathbf{K}_q^T\mathbf{K}_q\mathbf{P}_s$$
$$\mathbf{M}_{p.s} = \mathbf{P}_s^T\mathbf{K}_q^T\mathbf{K}_q\mathbf{P}_p.$$

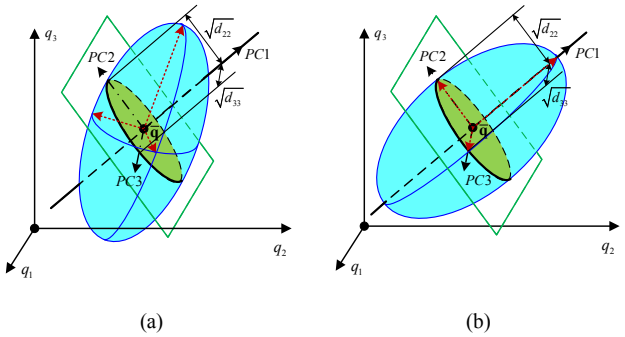

Fig. 7. Compliance ellipsoid matches to PCA. (a) Meet Condition 1. (b) Meet Condition 1 and 2 simultaneously.

Then, the conditions are given for mechanical compliance matching:

1) If $\mathbf{M}_s$ is diagonal matrix and its diagonal element is inversely proportional to variance of corresponding principal components,

$$\begin{cases} m_{sij} = 0, \quad i \neq j, \quad i, j = 1,...,l \\ \dfrac{1}{m_{s11}} : ... : \dfrac{1}{m_{sll}} = d_{s1} : ... : d_{sl} \end{cases}, \tag{9}$$

l is dimension of secondary movement subspace, then compliance ellipsoid matches constant density ellipsoid in secondary movement subspace.

2) When $\mathbf{M}_{p.s}$ is null matrix,

$$\mathbf{M}_{p.s} = \mathbf{0}, \tag{10}$$

the compliance between primary movement subspace and secondary movement subspace is decoupled.

Condition 1 is the basic requirement to realize compliance matching, guaranteeing mechanical compliance matching the sports statistics in secondary movement subspace, showed as Fig. 7(a). Condition 2 can achieve mechanical compliance decoupling primary and secondary motion. It is the best case to meet Condition 1 and 2 simultaneously, showed in Fig. 7(b), where $\mathbf{M}_p$ is a block diagonal matrix and the elastic elements serial to actuators do not influence mechanical compliance matching to high-order PCs, such as PCA finger showed in Fig. 5.

$\mathbf{M}_p$ is ignored for strictly movement refactoring, but it is better that $\mathbf{M}_p$ is full rank especially in the condition of the low precision of the control and sensor, which is equivalent to the compliance of actuators.

The above conditions can be used as the design criterion for compliant underactuated hands, which will be used in the design of parameters soon afterwards.

C. Simplify to implement

The finger model in Fig. 5 meets above two conditions, but embedded in humanoid robot hand using conventional manufacturing technology is a difficult problem. We simplify the mechanical structure to implant into the artificial limb.

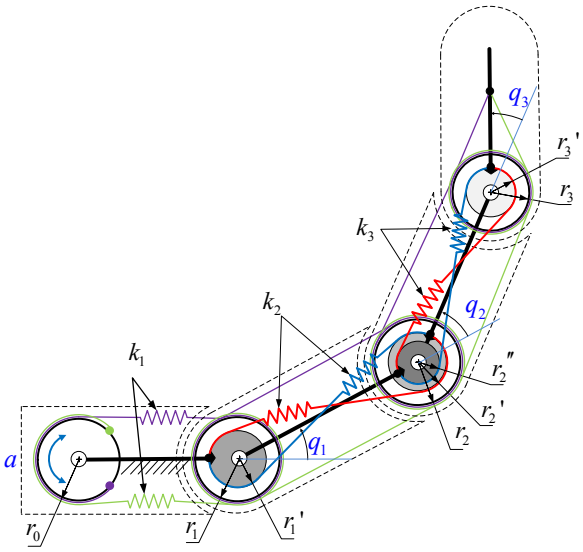

Fig. 8. The schematic diagram of improved mechanical structureform the single-actuator PCA finger.

The mechanical structure is improved through shortenning the compliance coupling chain of joints to adjacent joints, showed in Fig. 8, where k_i is the resultant stiffness of two antagonistic springs, corresponding deformation of springs denoted as Δ_i. q_i is defined as 0 when the finger was straight and in the plane of the palm. The kinematic variables a, Δ_i are defined as 0 when $\mathbf{q}=\bar{\mathbf{q}}$. The relations of the fingers kinematic variables are expressed as:

$$\begin{cases} a\cdot r_0-\Delta_1=r_1(q_1-\bar{q}_1)+r_2(q_2-\bar{q}_2)+r_3(q_3-\bar{q}_3) \\ \Delta_2=r_1'(q_1-\bar{q}_1)-r_2'(q_2-\bar{q}_2) \\ \Delta_3=r_2''(q_2-\bar{q}_2)-r_3'(q_3-\bar{q}_3) \end{cases} . \quad (11)$$

Under free motion, $\Delta_i=0, i=1,2,3$, the trajectory of primary motion is a straight line in joint space ,

$$\begin{bmatrix} q_1 \\ q_2 \\ q_3 \end{bmatrix} = \frac{r_0 a}{r_1 r_2' r_3' + r_1' r_2 r_3' + r_1' r_2'' r_3} \begin{bmatrix} r_2' r_3' \\ r_1' r_3' \\ r_1' r_2'' \end{bmatrix} - \begin{bmatrix} \bar{q}_1 \\ \bar{q}_2 \\ \bar{q}_3 \end{bmatrix} . \quad (12)$$

When the actuator is fixed, the changes of joint angles are closely related to the deformation of elastic elements. The elastic potential energy of the finger is expressed as

$$E=\frac{1}{2}k_1\Delta_1^2+\frac{1}{2}k_2\Delta_2^2+\frac{1}{2}k_3\Delta_3^2 \quad (13)$$

Calculating second order partial derivatives of the potential energy with respect to joint angles, the stiffness matrix can be obtained as,

$$\mathbf{K}_q=\frac{\partial^2 E}{\partial \mathbf{q}^2}$$

$$=\begin{bmatrix} k_1 r_1^2+k_2 r_1'^2 & k_1 r_1 r_2-k_2 r_1' r_2' & k_1 r_1 r_3 \\ k_1 r_1 r_2-k_2 r_1' r_2' & k_1 r_2^2+k_2 r_2'^2+k_3 r_2''^2 & k_1 r_2 r_3-k_3 r_2'' r_3' \\ k_1 r_1 r_3 & k_1 r_2 r_3-k_3 r_2'' r_3' & k_1 r_3^2+k_3 r_3'^2 \end{bmatrix}$$

Now, the constraint of parameter design is presented. At first, the primary motion is driven by the actuator, so the constraint equations making the trajectory as (12) colinear with PC1, are given,

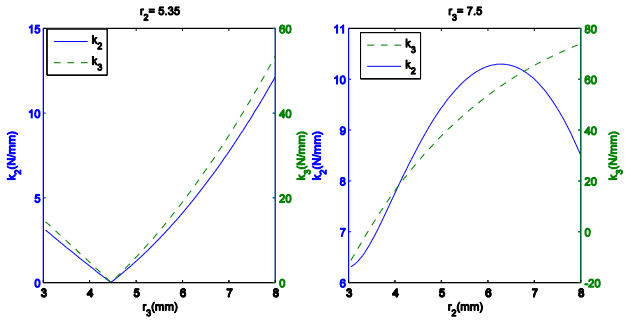

Fig. 9. A tip of the relationship among r_2, r_3, k_2, k_3, given other parameters.

$$\begin{cases} \frac{r_2'}{r_1'}=\frac{p_{11}}{p_{12}} \\ \frac{r_3'}{r_2''}=\frac{p_{12}}{p_{13}} \end{cases} \quad (14)$$

According to Condition 1, there are two constraint equations,

$$m_{p32}=0 \quad , \quad (15)$$

$$\frac{1/m_{p22}}{1/m_{p33}}=\frac{d_2}{d_3} . \quad (16)$$

Condition 2 could not be satisfied usually in this mechanism because of the limited capacity to regulate the compliance ellipsoid via parameter design.

There are 4 constraint equations and 10 parameters, except for actuator pulley radius r_0 . Given $r_2'=6mm$ and $r_2''=4mm$, we can obtain $r_1'=8.0mm$ and $r_3'=4.8mm$ via (14). Then, given $k_1=40N/mm$ and $r_1=4.0mm$, the relationship of r_2, r_3, k_2, k_3 described in (15) and (16), are showed in Fig. 9.

A group of parameters, which can be achieved in engineering, is chosen in the constraint relations,

$r_2=4.9mm, r_3=6.8mm$

$k_2=6.5N/mm, k_3=24.2N/mm$

From the design process, the constraint equations give only the relationship among parameters, such as Fig. 9. The optimal parameter values can be obtained in other ways, such as feasibility of manufacturing, force and stability during grasp.

A view of the latest-design finger prototype is presented In Fig. 10(a), whose basic size is *18mm*×*14mm*×*106mm* and is embedded in a prosthesis prototype (Fig. 10(b)).

IV. Conclusions and Future Works

Abundant human hand grasping behavior can be decoupled in the PCA coordinate system, significantly distinguishing the primary and secondary direction of movements. The statistics characteristic of human finger motion data can be more intuitively reflect this primary and secondary laws of motion via visualizations, and then guide the mechanical design of humanoid hand.

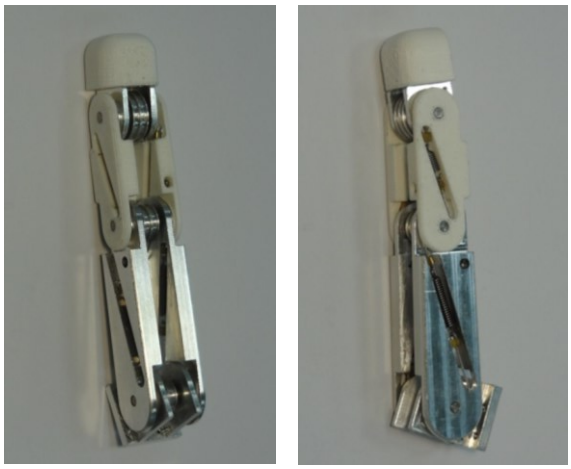

(a)

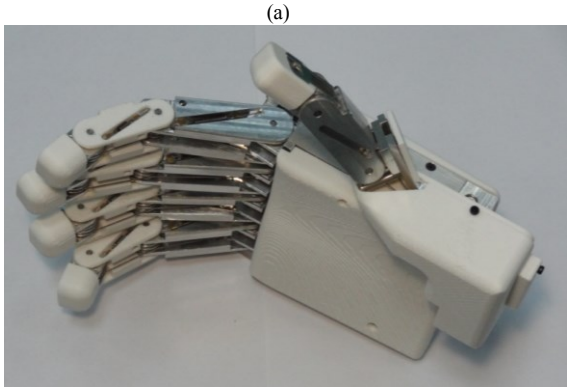

(b)

Fig. 10. (a) The latest-design finger prototype. (b)The finger is emdedded in a prosthesis prototype.

Primary movement reflects the overall finger movement, achieved through actively driven by acuators; the secondary movement information is implicated in the mechanical compliance, without loss of statistical information of human hand motion while decreasing controlling complexity and manufacturing costs of robotics hand.

The novel finger mechanism presented in the paper goes ahead free movement without overcoming the resistance of the elastic element, and is arranged the smallest elastic restraint. The mechanical behavior and grasp ability of the mechanism can be explored further.

For the mechanical reproduction of human hand grasping behavior, we propose the mechanical compliance matching method which has certain universality and will be extended to parameter design of compliance underactuated hands.

REFERENCES

[1] M. Santello, M. Flanders, and J. F. Soechting, "Postural Hand Synergies for Tool Use," *The Journal of Neuroscience,* vol. 18, pp. 10105-10115, 1998.

[2] M. Santello, M. Flanders, and J. F. Soechting, "Patterns of Hand Motion during Grasping and the Influence of Sensory Guidance," *The Journal of Neuroscience,* vol. 22, pp. 1426-1435, 2002.

[3] M. Ciocarlie, C. Goldfeder, and P. Allen, "Dimensionality reduction for hand-independent dexterous robotic grasping," in *IEEE/RSJ International Conference on Intelligent Robots and Systems*, 2007, pp. 3270-3275.

[4] C. Y. Brown and H. H. Asada, "Inter-finger coordination and postural synergies in robot hands via mechanical implementation of principal components analysis," in *IEEE/RSJ International Conference on Intelligent Robots and Systems*, 2007, pp. 2877-2882.

[5] M. Gabiccini, A. Bicchi, D. Prattichizzo, and M. Malvezzi, "On the role of hand synergies in the optimal choice of grasping forces," *Autonomous Robots,* vol. 31, pp. 235-252, 2011.

[6] M. G. Catalano, G. Grioli, A. Serio, E. Farnioli, C. Piazza, and A. Bicchi, "Adaptive synergies for a humanoid robot hand," in *Humanoid Robots (Humanoids), IEEE-RAS International Conference on*, 2012, pp. 7-14.

[7] A. M. Dollar and R. D. Howe, "Joint coupling design of underactuated hands for unstructured environments," *The International Journal of Robotics Research,* vol. 30, pp. 1157-1169, 2011.

[8] D. G. Kamper, E. G. Cruz, and M. P. Siegel, "Stereotypical Fingertip Trajectories During Grasp," *Journal of Neurophysiology,* vol. 90, pp. 3702-3710, 2003.

[9] C. R. Mason, J. E. Gomez, and T. J. Ebner, "Hand Synergies During Reach-to-Grasp," *Journal of Neurophysiology,* vol. 86, pp. 2896-2910, 2001.

[10] J. R. Napier, "The Prehensile Movements of the Human Hand," *Journal of Bone & Joint Surgery, British Volume,* vol. 38-B, pp. 902-913, 1956.

[11] M. R. Cutkosky, "On grasp choice, grasp models, and the design of hands for manufacturing tasks," *Robotics and Automation, IEEE Transactions on,* vol. 5, pp. 269-279, 1989.

[12] T. Feix, R. Pawlik, H.-B. Schmiedmayer, J. Romero, and D. Kragi´, "A comprehensive grasp taxonomy," in *in Robotics, Science and Systems Conference: Workshop on Understanding the Human Hand for Advancing Robotic Manipulation*, 2009.

[13] J. Z. Zheng, S. De La Rosa, and A. M. Dollar, "An investigation of grasp type and frequency in daily household and machine shop tasks," in *IEEE International Conference on Robotics and Automation (ICRA)*, 2011, pp. 4169-4175.

[14] I. M. Bullock, J. Z. Zheng, S. D. L. Rosa, C. Guertler, and A. M. Dollar, "Grasp Frequency and Usage in Daily Household and Machine Shop Tasks," *Haptics, IEEE Transactions on,* vol. 6, pp. 296-308, 2013.

[15] T. F. Ian M. Bullock, and Aaron M. Dollar, "Finding Small, Versatile Sets of Human Grasps to Span Common Objects," in *IEEE International Conference on Robotics and Automation (ICRA)*, Karlsruhe, Germany, 2013, pp. 1068-1075.